素子材料特論
第2授業

Li-ion電池負極(I)

1. Li-ion電池および負極
2. 黒鉛系負極

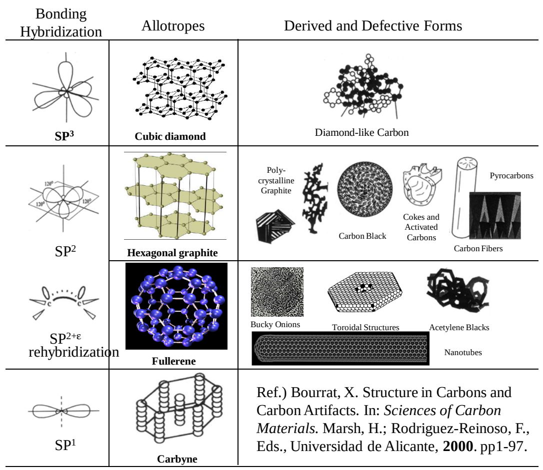

Carbon Allotropes

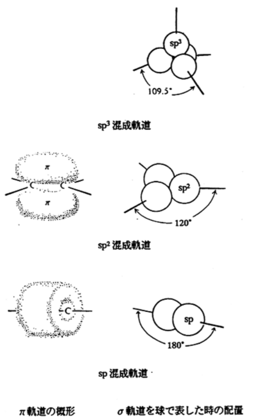

図-1 炭素の混成軌道

表-1 各種炭素－炭素結合の結合解離エネルギーと結合距離 1)

化合物	結合解離エネルギー (kcal/mol)	結合距離 (Å)
H_3C-C_3H	88	1.53
H_2C＝C_2H	163	1.34
HC≡CH	198	1.21

表-2 炭素同素体の種類 3)

結合の種類	配位数	炭素同素体
sp	2	カルビン (ポリイン, クムレン)
sp^2	3	グラファイト (六方晶, 菱面体晶)
		フラーレン (C_{60}, C_{70}, バッキイチューブなど)
sp^3	4	ダイヤモンド (立方晶, 六方晶, 菱面体晶*)
		ダイヤモンド多形体 (6H, bc-8*など)
		ダイヤモンドライクカーボン (DLC), i-カーボン
イオンまたは	6	単純立方晶*, β-スズ型*
金属的	8	体心立方晶*
	12	面心立方晶*, 六方最密充填*

* 実

表-4 Ⅳ族 sp^3 立方晶体の性質 6)

性質	ダイヤモンド	β-SiC	Si
格子定数 (Å)	3.567	4.358	5.430
密度 (g/cm^3)	3.515	3.216	2.328
熱膨張率 ($\times10^{-6}$/℃)	1.1	4.7	2.6
融点 (℃)	4000	2540	1420
バンドギャップ (eV)	5.45	3.0	1.1
キャリア移動度 ($cm^2/(V \cdot S)$)			
電子	2200	400	1500
ホール	1600	50	600
熱伝導率 ($W/(cm \cdot K)$)	20	5	1.5
硬度 (kg/mm^2)	10000	3500	1000

Molecular structures of graphite

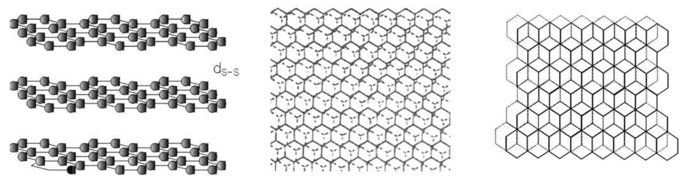

(a) Basic Structure of Graphite

(b) Turbostratic structure (low crystallinity)

(C) Graphitic structure (high crystallinity)

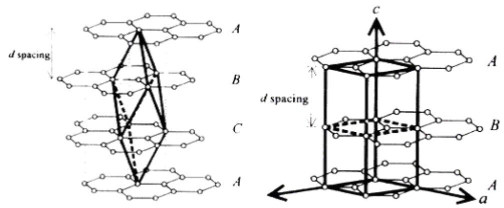

Characteristics of carbons

- Thermal stability
- High thermal and electric conductivities
  SWNT, Diamond : 4000 W/mK, K-11
  carbon fiber: 1100 W/mK
- Small heat expansion
- High thermal shock properties
- High chemical stability
- Abrasion and lubricant properties
- High mechanical properties

33

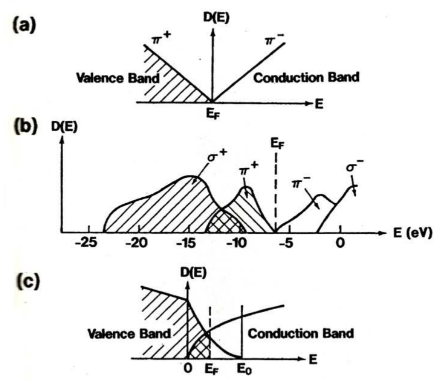

電子の状態密度*D*(*E*)のエネルギー*E*依存：2次元黒鉛に対するフェルミエネルギーE_F近傍のπ電子の電子状態状態分布（a），黒鉛の全エネルギー領域における電子状態分布密度分布（b），および黒鉛のE_F近傍のπ電子の状態密度分布（c）

Carbon is key element for Batteries !!

①Li-ion

[High capacity]

(+) : LiCoO2
(-) : Carbon(Graphite)
Conductor :Carbon

②Dry Battery

[Cheap]
[Easy Available]

(+) : MnO2
(-) : Zn
Conductor :Carbon

③Ni-MH

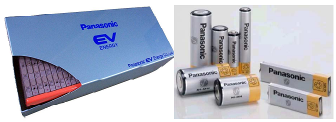

[High power]
[Total balance]

(+) : (Ni-Co)$(OH)_2$
(-) : Mm(Ni-Mn-Al-Co)$_5$
substrate:Nickel and Carbon

25/24

Applications and necessity of Li-ion battery

Energy storage system in smart grid

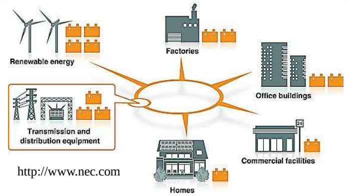

http://www.nec.com

Power source of electric vehicles

ICE

< Toyota Camry >

Electric motor

< Toyota RAV4 EV >

Energy density of various rechargeable batteries

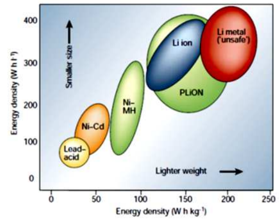

J.M. Tarascon, M. Armand, Nature 414 (2001) 359.

Li-ion battery is paid much attention as power sources of ESS and electric vehicles in a variety of rechargeable batteries.

ICE : Internal combustion engine, ESS : Energy storage system

8

Global market and requirements of Li-ion battery

Global market of Li-ion battery in ESS

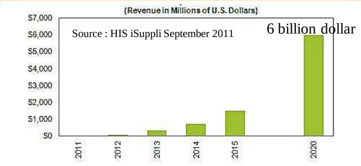

Global market of Li-ion battery in EV

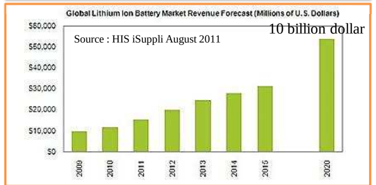

Requirements of Li-ion battery as power sources of ESS and EV

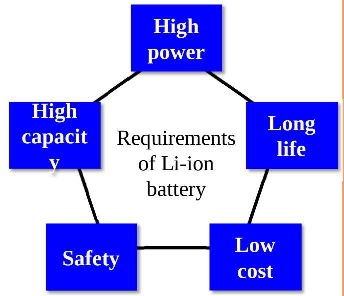

9

Carbon Electrode for Li-ion Battery

- **Graphite electrode is currently established.**
  - ➢ Low cost with cheaper natural graphite
  - ➢ Limited capacity less than 372 mAh/g
  - ➢ Limited power density

Larger power density for hybrid vehicle
➔ Glassy carbon with small crystalline unit (Low Cond.)
Thinner carbon nanofiber

Larger capacity
➔ Glassy carbon with large inner surface
Si or Sn family (Large volumetric change at Ch/Disc)
⇨ **Functional nano-composites**

Roles of Carbon for Anode of Li-ion Batteries

- Anodic Electrode to Hold Reduced Li-ion
  Intercalation → Graphite
  Surface Electron Transfer into Sealed Void
  → Carbon
- Electron Conductive Material
  Anodic Carbon and Cathodes Material
- Expansion Moderation
  Holding and Release of Ion Is Accompanied with Volumetric Charge
  Larger Capacity per Volume → Larger Expansion

電池負極物質

- 電池の中で還元剤として機能

自身が酸化（イオン化）し、電解質に溶解することで負極は負に帯電する。活量=1の水溶液中、標準状態における標準水素電極に対するその電位は標準電極電位E0と呼ばれ、元素ごとで表に示す異なる値を取る。

E0 = - ΔG/nF (イオン化傾向、真空中で陽イオンになりやすさ)

表1　代表的な金属元素の標準電極電位と第1イオン化エネルギーの相関

電極	放電反応	ギブスエネルギー	標準電極電位	イオン化エネルギー
Li	$Li \rightarrow Li^{+} + e^{-}$	−293.31 kJ/mol	−3.045 V	520 kJ/mol
K	$K \rightarrow K^{+} + e^{-}$	−283.27 kJ/mol	−2.925 V	419 kJ/mol
Ca	$Ca \rightarrow Ca^{2+} + 2e^{-}$	−553.58 kJ/mol	−2.866 V	590 kJ/mol
Na	$Na \rightarrow Na^{+} + e^{-}$	−261.9 kJ/mol	−2.714 V	496 kJ/mol
Mg	$Mg \rightarrow Mg^{2+} + 2e^{-}$	−454.8 kJ/mol	−2.363 V	738 kJ/mol
Al	$Al \rightarrow Al^{3+} + 3e^{-}$	−485 kJ/mol	−1.662 V	578 kJ/mol
Zn	$Zn \rightarrow Zn^{2+} + 2e^{-}$	−147.06 kJ/mol	−0.763 V	906 kJ/mol
Fe	$Fe \rightarrow Fe^{2+} + 2e^{-}$	−78.9 kJ/mol	−0.44 V	759 kJ/mol
H	$H \rightarrow H^{+} + e^{-}$	0 kJ/mol	0 V	1,312 kJ/mol
Cu	$Cu \rightarrow Cu^{2+} + 2e^{-}$	65.49 kJ/mol	0.337 V	745 kJ/mol
Ag	$Ag \rightarrow Ag^{+} + e^{-}$	77.1 kJ/mol	0.7991 V	731 kJ/mol

地殻中の各元素の存在比

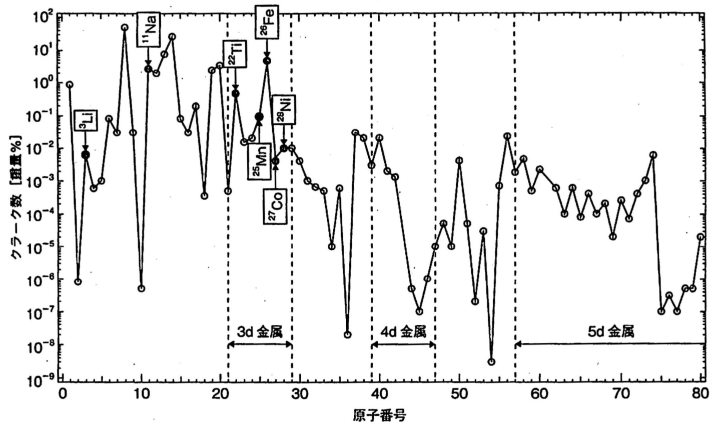

Li2次電池における負極材の研究動向

1. Li金属負極：
- 還元力の強さが仇となり、殆どの電解液を還元分解してしまう問題点あり。
- 還元の際、Dendrite結晶状として還元
- モリエナジー（カナダ）1989年、NTT形態で内部短絡事故
2. Carbon電極
- 1991年SONYが採択、Li-ion電池化、世界初
- C6Li, 372 mAh/g
3. Si, Sn系、チタニア系、バナディウム系…

Li-ion Battery Road

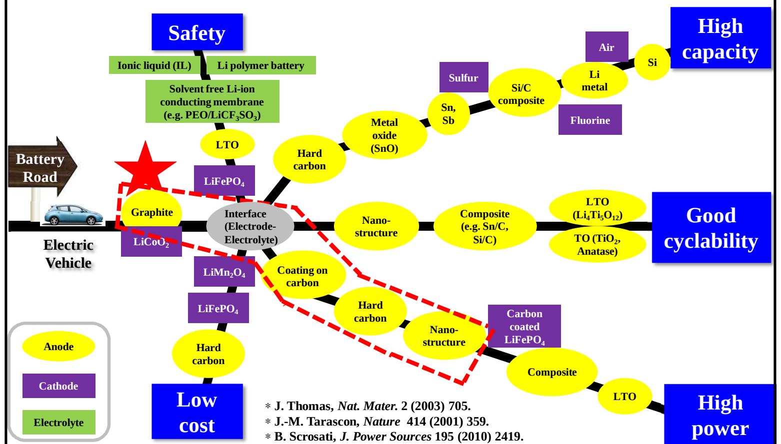

* J. Thomas, *Nat. Mater.* 2 (2003) 705.
* J.-M. Tarascon, *Nature* 414 (2001) 359.
* B. Scrosati, *J. Power Sources* 195 (2010) 2419.

15

Ch./Dis. Principle of Li-ion 2nd Batteries

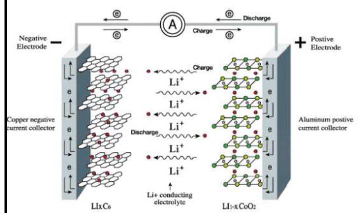

Anodic Materials for Li-ion 2nd Batteries

	Carbon	Si alloys	Li alloys
Theoretical Cap.(mAh/g)	372 (LiC_6)	4200 ($Li_{4.4}Si$)	3860
Present Stage	Commercialized	Developing	Developing
Merit	Low Cost Good Cycle Life Good Chemical Stability	High Capacity	High Capacity
De-merit	Low Rate Capability	High Volume Expansion ⇒ Bad Cycle	Strong Reaction ⇒ Bad Cycle & Thermal Stability
Materials	Graphite, Soft/Hard carbon	-	-
User	Sanyo, Matsushita, STC, A&T Battery, Shin-Kobe, GS, Moli, Mitsubishi, Sony, SDD, Hitachi Maxcel, LG Chem.	-	-

Characteristics and materials of 2nd Batteries

Ref. KISTI, Materials for 2nd Batteries (2004/06)

		Ni-Cd	Ni-MH	Li-ion	Li polymer
Cathodic material		NiOOH	NiOOH	LiMO2	LiMO2
Anodic material		Cd	MH	Carbon	Carbon
Electrolyte		KOH/H2O	KOH/H2O	LiX/Organic Solution	LiX/Polymer electrolyte
Operating voltage(V)		1.2	1.2	3.6	3.6
Cycle		1000	1000	1200	1000
Self discharge rate (%/month)		-	20~25	< 10	≪ 10
Environmental pollutant		Yes	Yes	No	No
Energy density	Per weight (Wh/kg)	-	65	120	100
	Per volume (Wh/L)	160	240	280	220
Manufacturing company		Sanyo, Toshiba	Matsushita, Sanyo, Toshiba	Sony, Sanyo, Matsushita	Valence, Ultralife

Mechanism of charge & discharge

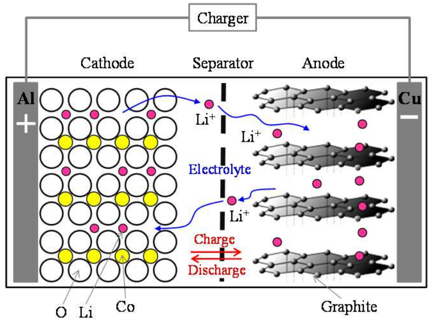

Cathode : $LiCoO_2 \leftrightarrow CoO_2 + Li^+ + 2e^-$

Anode : $C_6 + Li^+ + e^- \leftrightarrow LiC_6$

Overall : $LiCoO_2 + C_6 \leftrightarrow CoO_2 + LiC_6$

Carbon materials of LIB

	Precursor	Advantages	Disadvantages
Graphite (over 2800°C)	Natural / Artificial graphite MCMB, Needle cokes VGCF	Low discharge potential (≈ 0.2V) Long cycle life	Low discharge capacity (372 mAh/g) Poor rate performance High cost
Soft Carbon Graphitizable carbon (600~800°C)	MCMB Meso phase pitch Green cokes	High capacity (700~1000mAh/g) Low cost	High discharge potential (≈ 1.0V) High irreversible capacity Poor cycle stability
Hard Carbon Non-graphitizable carbon (1000~1400°C)	Thermosetting polymer Glassy carbon, Coal Organic material Stabilized isotropic pitch	High capacity (400~700mAh/g) High rate performance Low discharge potential (≈ 0.1V) Low cost	Large irreversible capacity

Characteristics of Carbon Material

HTT ↔ Resistance

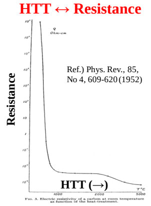

Li content ↔ d-spacing

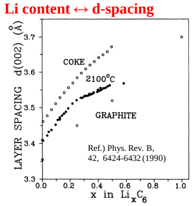

HTT ↔ Capacity

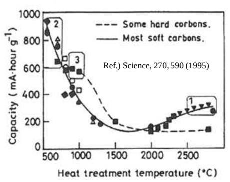

Structural mechanism of carbon

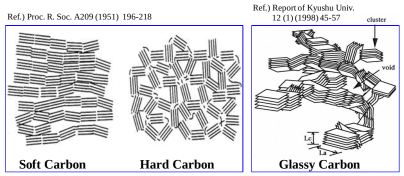

Charge-Discharge Profile

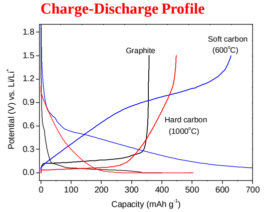

Lithium Ion Battery, Electrode

Lithium ion insertion sites of carbon

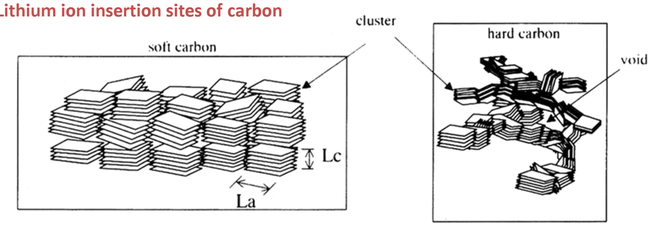

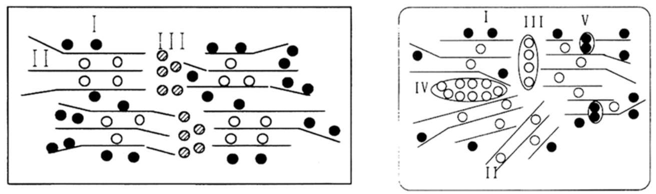

Typical Properties of Synthetic Graphites

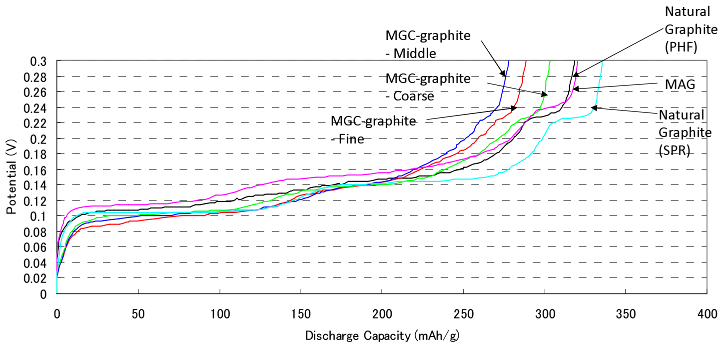

GraphiteとGraphene

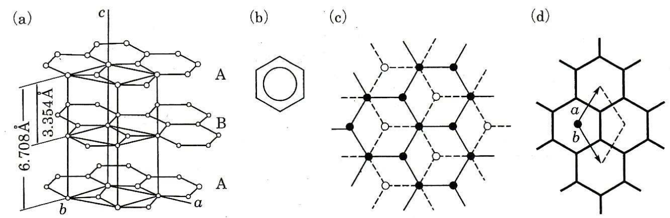

図4.2　グラファイトの構造

(a) グラファイトの結晶構造．ABA 様式で積層している．(b) ベンゼン．(c) c 軸方向の上方から 2 枚面の重なりを見たもの．●が上の面の炭素原子で，○が下の面の炭素原子を表す．(c) ab 面の構成．単一の ab 面（グラフェン面）だけなら，単位セルは菱形の部分で，2 個の炭素原子を含む．ab 面の並進長さは，$|a|=|b|=2.462$ Å.

22

炭素の結晶構造パラメータ

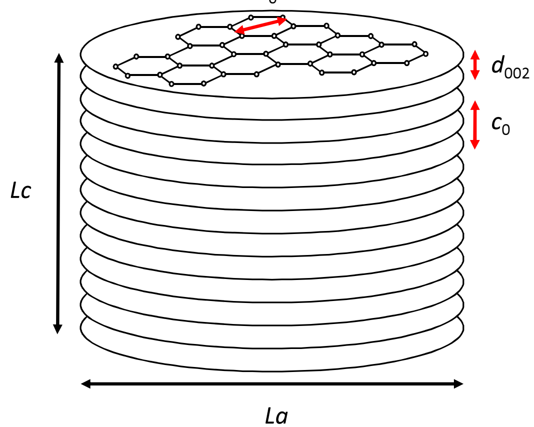

結晶面と面間隔の関係

(002)面と$d_{(002)}$

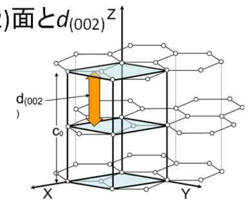

(110)面と$d_{(110)}$

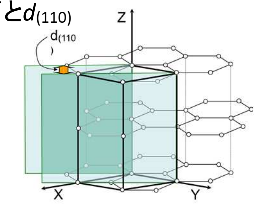

(112)面と$d_{(112)}$

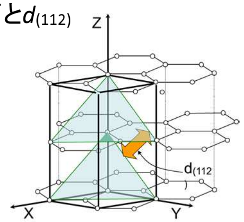

Graphiteの構造

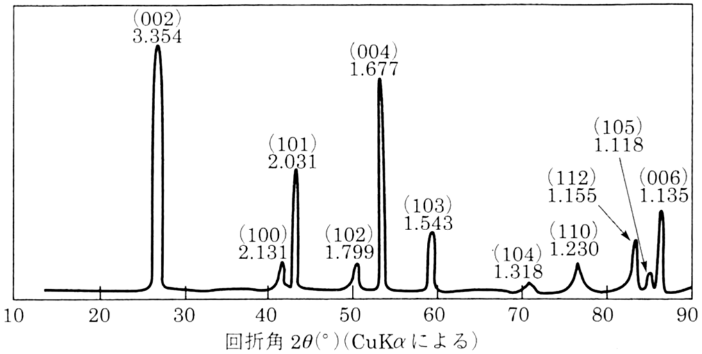

図4.4 グラファイトの X 線回折パターン

25

黒鉛の電子構造

32

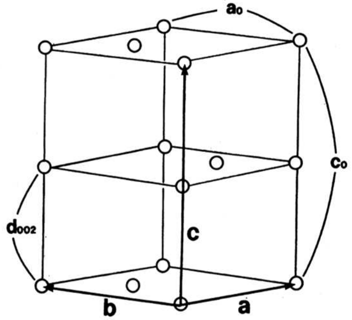

最隣接原子間距離:0.1421nm
第2隣接原子間距離:0.2461nm
層間距離:0.3354nm

黒鉛結晶の単位格子と格子定数a_0,c_0および基本格子ベクトル***a,b,c***

Graphiteの反応性

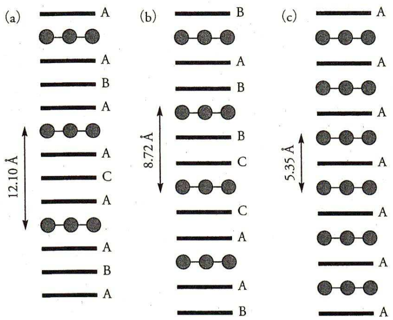

図4.6 カリウムをインターカレートとした GIC のステージ構造

実線はグラファイトの *ab* 面で, A, B, C はその積層様式. 灰色の丸印はカリウム原子.
(a) KC_{36} (ステージ3), (b) KC_{24} (ステージ2), (c) KC_8 (ステージ1).

GICでは、HOバンドの頂上から電子が引き抜かれることによって正孔が注入されたり、LUバンドの底に余剰電子が与えられたりするので、フェルミ状態の密度が増加して導電性が上がる。

27

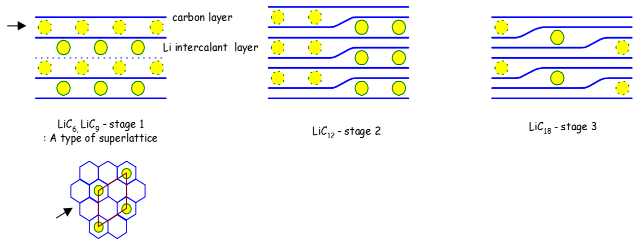

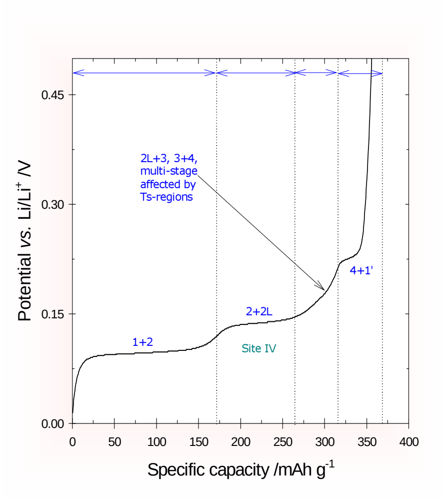

Voltammetric behavior of grpahite

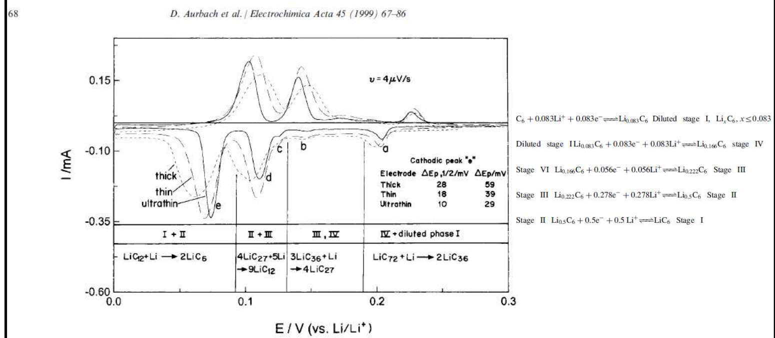

Fig. 1. Typical voltammetric behavior of graphite electrodes at a very slow scan rate, $v = 4$ μV/s in EC-DMC 1:3/LiAsF$_6$ solution. (Graphite flakes, KS-6, Timcal). Ultrathin, thin and thick electrodes correspond to submicronic (0.16 mg/cm^2, see preparation procedure in Refs. [5,9]), 10 microns (3.3 mg/cm^2), and 140 μm (12 mg/cm^2), respectively. The current for the thin and ultrathin electrodes was normalized with that of the thick electrodes according to their mass ratios in order to have the 3 CV on the same scale. The electrode area was 2.4 cm^2 for the thin and the ultrathin, and ≈0.2 cm^2 for the thick electrode.

Design and Its Thermal Change of Aromatic Stacking

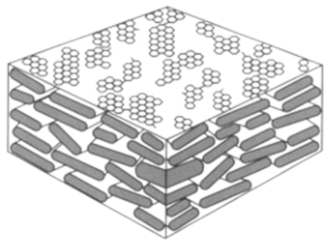

Molecular Models

Spider Wedge Stacking of mesophase pitch
(Zimmer et al. Advances in Liquid Crystal, New York, 1982, 5)

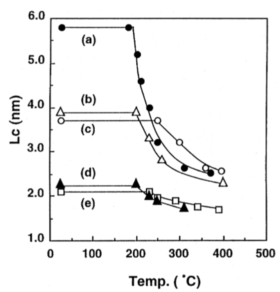

Melt-XRD analysis

Change in Lc of mesophase pitch at higher temperature; (a) methylnaphthalene-derived pitch; (b) petroleum-derived mesophase pitch; (c); coal tar derived-mesophase pitch; (d) naphthalene-derived mesophase pitch; (e) anthracene-derived mesophase pitch
(Korai et al. Carbon, 1992, 30, 1019)

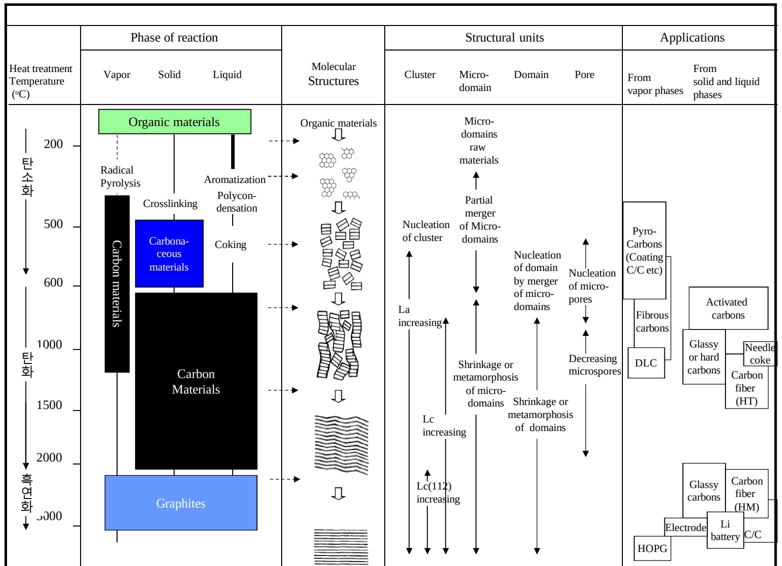

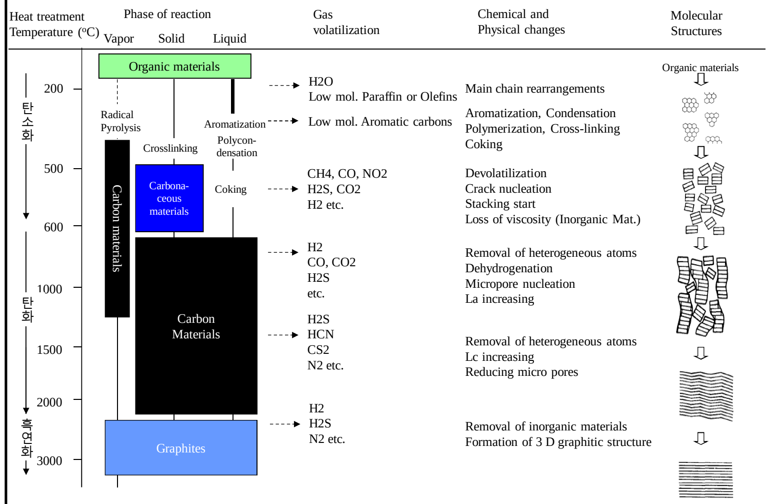

Franklin's Models of Carbon Structures

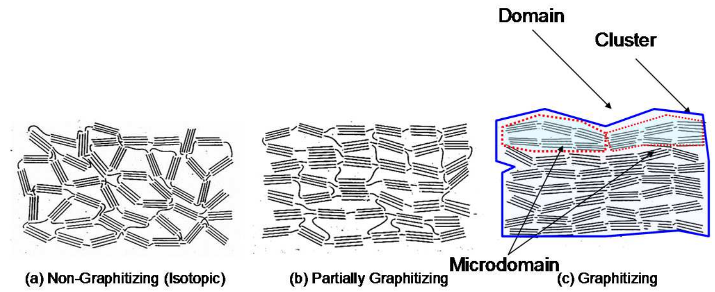

有機物の加熱による変化

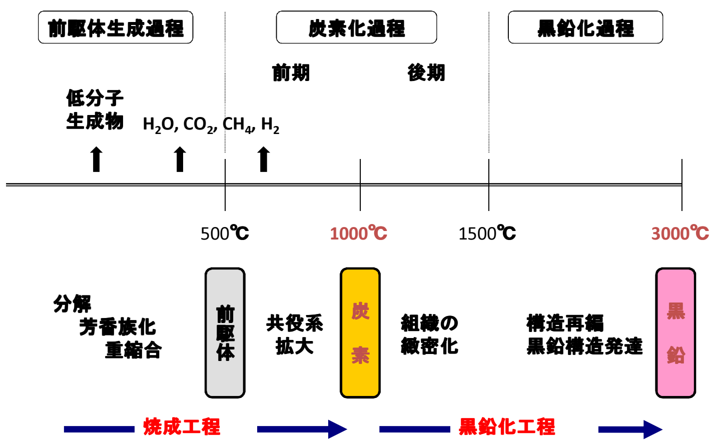

熱処理温度による結晶構造変化

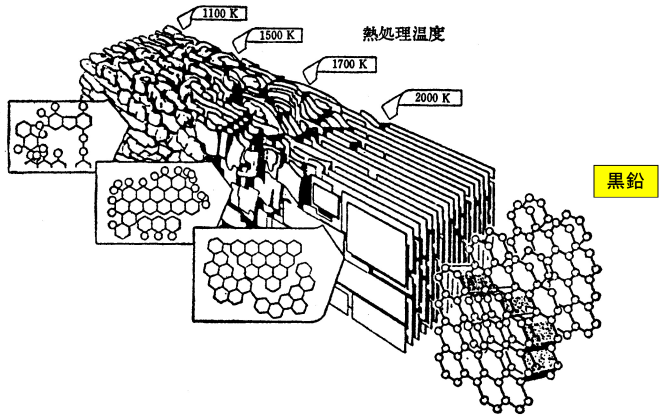

Structure of Needle Coke

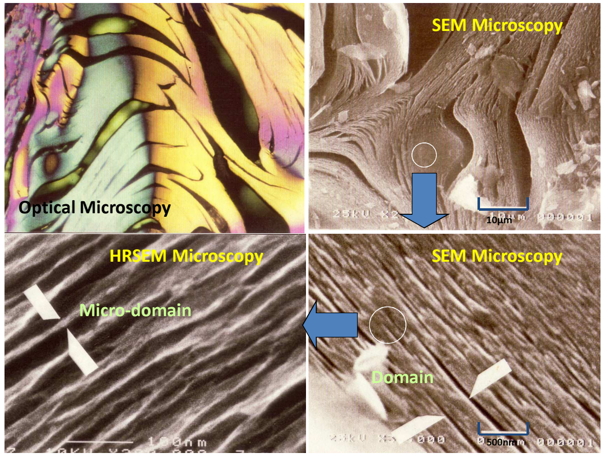

Nanoscopic Structure of Mesophase Pitch Based Carbon Fiber

Problem: Low Compressive Strength > Restriction of CFRP Application

Factor: Size and Distribution of Micro-domain

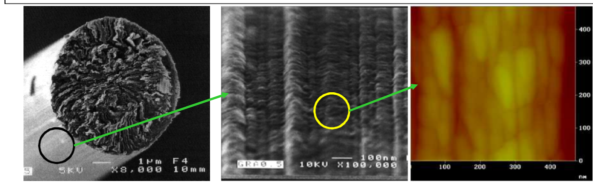

Pleat Structure > Homogeneous / Small > Increasing Compressive Strength

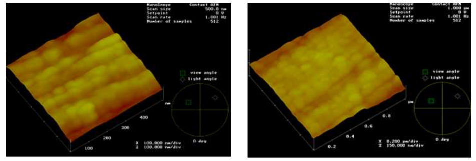

Structure of MCMB

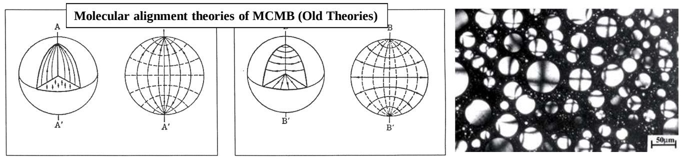

(a) Brooks-Taylor Type | (b) Honda Type | **Optical Micrograph of MCMB in Isotropic Matrix**

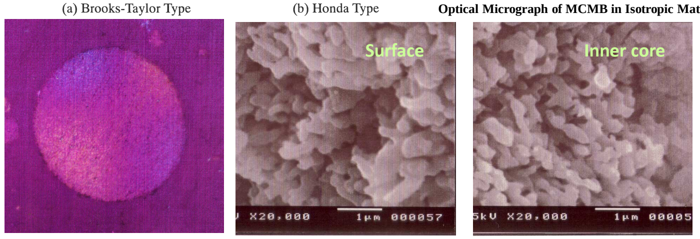

Optical Micrograph of PI of AR pitch derived MCMB | SEM Photograph of PI of AR pitch derived MCMB | SEM Photograph of PI of AR pitch derived MCMB

TEM Images of Hongye Anthracites Heat Treated at Various Temperatures

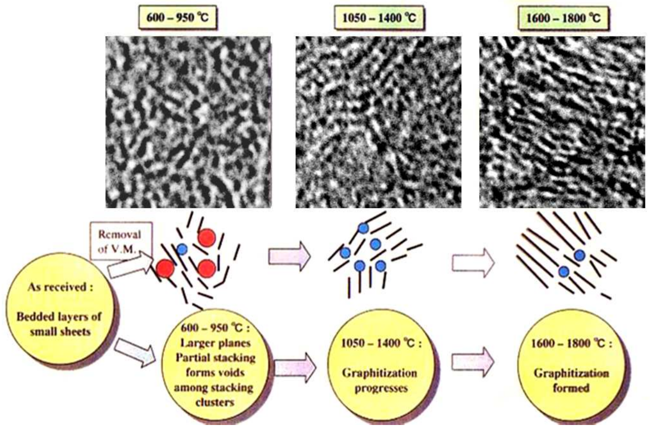

Franklin's Models of Carbon Structures

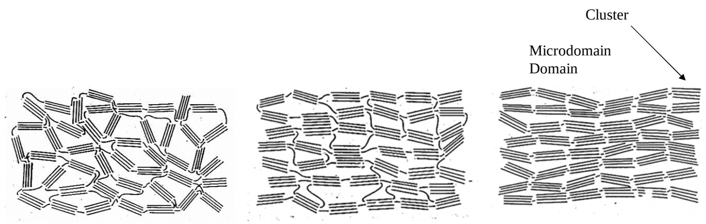

(a) Non-Graphitizing (Isotopic) (b) Partially Graphitizing (c) Graphitizing

Structural Models of Glassy Carbon Heated at High Temperature

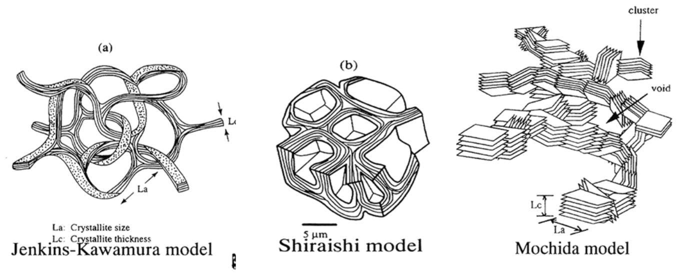

Structural Hierarchy in Mesophase Pitch

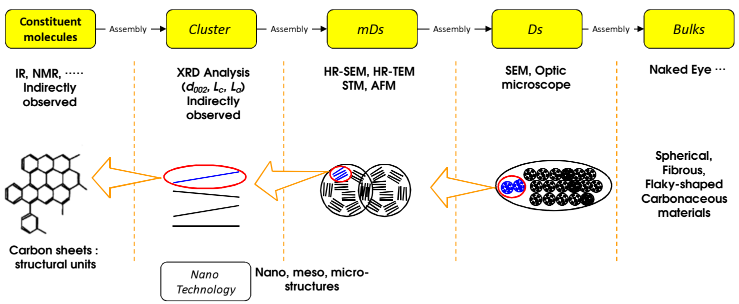

MCMB

Lot		容量(mAh/g, 0~1.5V)			Dcap. (0~0.5V)	低電圧特性 (0.5V/1.5V)(%)
		1cy	2cy	3cy		
600℃ 熱処理	ch	1497	440	368	124	38.5
	dis	396	342	321		
	効率(%)	26.5	77.6	87.2		
1200℃ 熱処理	ch	393	308	303	197	67.1
	dis	303	299	294		
	効率(%)	77.2	96.9	97.1		
1400℃ 熱処理	ch	359	295	289	198	69.7
	dis	291	288	284		
	効率(%)	81.1	97.6	98.3		
2000℃ 熱処理	ch	227	198	194	159	83.0
	dis	196	193	191		
	効率(%)	86.1	97.6	98.4		
2400℃ 熱処理	ch	298	262	259	238	93.2
	dis	258	258	256		
	効率(%)	86.6	98.5	98.8		
2800℃ 熱処理	ch	426	364	360	344	96.5

Previous study of Soft Carbon

Graphite has a limitation at capacity and power density, such reason enforced to develop other carbon materials like soft carbon and hard carbon

Ch-Dis Profile & SEM image

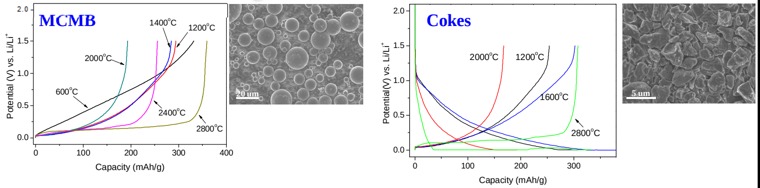

Structural change of Cokes

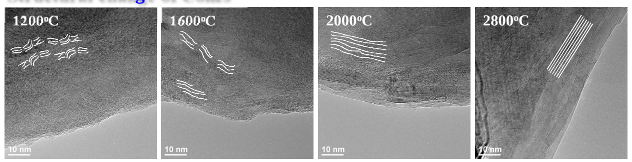

45

MCMB

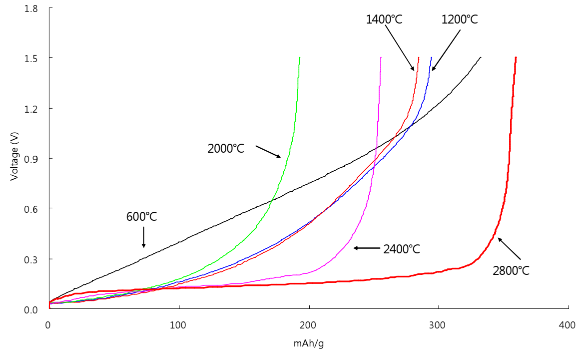

MCMB

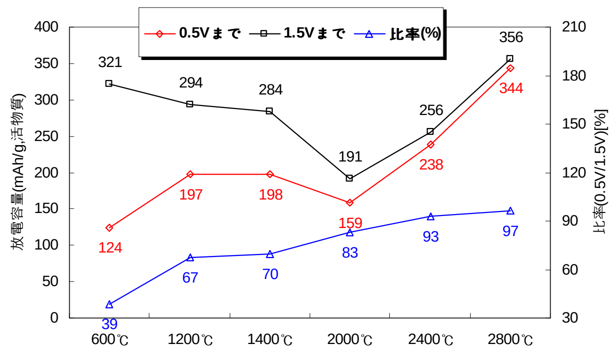

MCMB

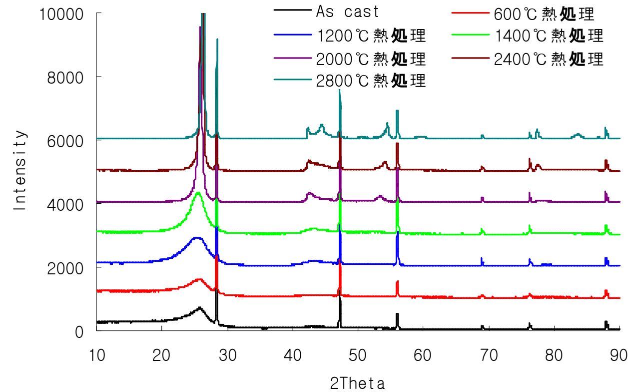

MCMB

	d_{002} (A)	Lc002 (nm)
As cast	3.4945	3.1
600℃ 熱処理	3.5138	3.1
1200℃ 熱処理	3.5278	4.1
1400℃ 熱処理	3.4876	6.8
2000℃ 熱処理	3.4280	35.44
2400℃ 熱処理	3.3887	53.70
2800℃ 熱処理	3.3628	122.0

MCMB

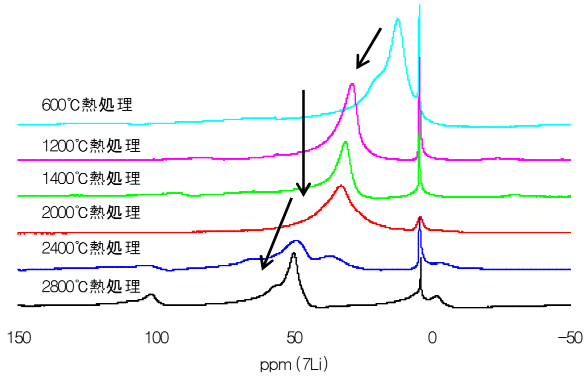

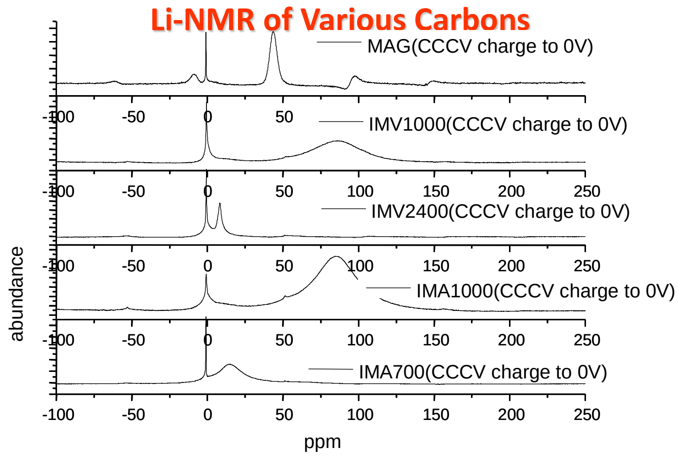

Discharging EVS Profiles of NC E Series

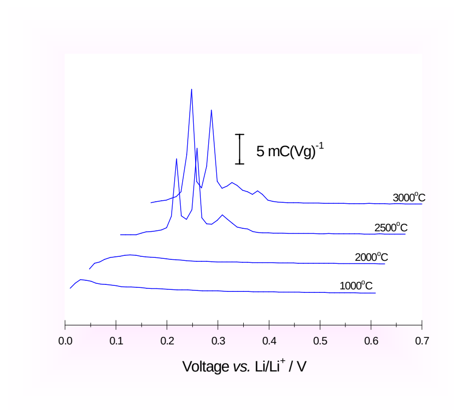

Discharging EVS Profiles of natural and synthetic graphites

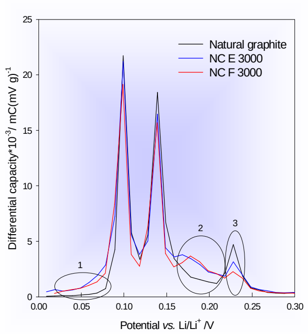

Roles of Carbon for Anode of Li-ion Batteries

- Anodic Electrode to Hold Reduced Li-ion
  - Intercalation → Graphite
  - Surface Electron Transfer into Sealed Void → Hard or Low Temperature Calcined Carbon
- Electron Conductive Material
  - Anodic Carbon and Cathode Material
- Expansion Moderator
  - Holding and Release of Ion Is Accompanied with Volumetric Charge
  - Larger Capacity per Volume → Larger Expansion
- Moderation and Control of SEI
  - Irreversible Charge → Surface Coating, Composite Structure

Typical Graphites

Natural Graphites

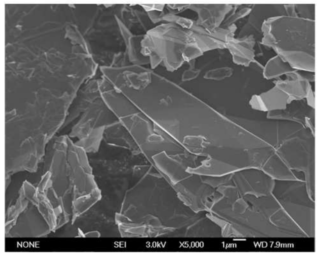

- **Cheap**
- **High graphitization degree**
- **Large Irreversible Capacity**
- **Relatively poor Cycle Life**
- **Poor Rate Capability**

Synthetic Graphites

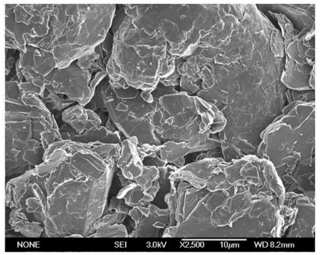

- **Good 1st cycle efficiency & Cycle Life**
- **Relatively high graphitization degree**
- **Poor Rate Capability**

(MAG; Hitachi Chemical Co.)

Surface Oxygen Functional Groups of AC

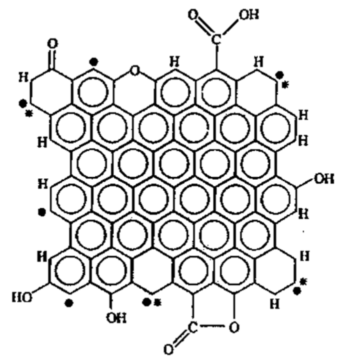

This structure is representative of an activated carbon with a crystallite width of 15 Å and an elemental analysis (by weight) of 87.5% C, 11.3% O, 1.2% H, ● represents an unpaired σ electron ; ●* represents an "in-plane σ pair" with * being a localized π electron. (Radovie)

SEM & TEM Images of PCNF Series

Ref.) S. Lim, et al. *J. Phys. Chem. B* 108 (5), 1533 – 1536 (2004)

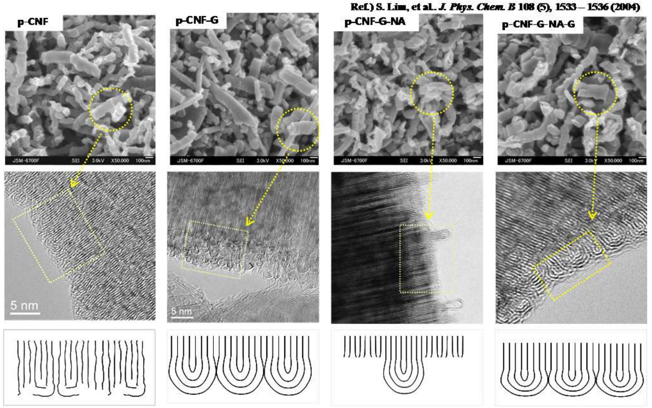

According to the graphitization degree, we found some difference at edge plane by TEM analysis

Basic study of solid electrolyte interphase (SEI)

Characteristics of SEI

- ➢Reduction of electrolyte components on anodes on initial charge
- → Irreversible capacity loss
- → Decrease of first-cycle coulombic efficiency
- ➢ Passage of Li-ion migration, but high electronic resistivity
- ➢Essential to determine the electrochemical properties and safety of Li-ion battery

< Schematic model of SEI formed on anodes >

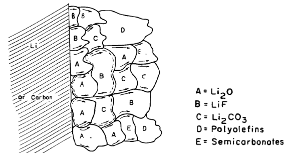

E. Peled et al., J. Electrochem. Soc. 144 (1997) L208

Previous researches on SEI

- ➢Focused on SEI formation behavior of cross section of HOPG However, the cross section of HOPG was composed of edge planes and basal planes.

< Cross section of HOPG >

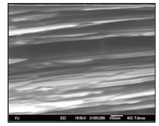

•T. Kim *et al.*, *Langmuir* 22 (2006) 9086.

Necessary to prepare well-defined edge and basal surfaces

Study on SEI formation behavior on well-defined edge and basal surfaces prepared by carbon nanofibers as a model material.

Preparation of PCNFs with well-defined surfaces

PCNF : Edge surface
- Fe catalyst
- CO:H_2 = 4:1 (total 2 L/min)
- 640˚C, 4 h

PCNF-G : Basal
- 2800˚C, 10 min

PCNF-G-NA : Edge
- 10 wt.% HNO_3
- 155˚C, 28 h

PCNF-B-G : Basal
- Ball-mill of PCNF with boric acid (5 wt% boron)
- 2800˚C, 10 min

PCNF-B-G-NA : Edge
- 10 wt.% HNO_3
- 155˚C, 28 h

PCNF : Platelet carbon nanofibers

* S. Lim *et al.*, *J. Phys. Chem. B* 108 (2004) 1533.

TEM images of PCNFs with well-defined surfaces

PCNF : Edge

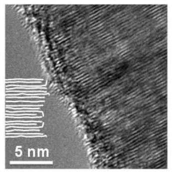

PCNF-G : Basal

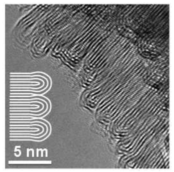

PCNF-G-NA : Edge

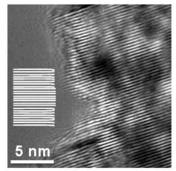

PCNF-B-G : Basal

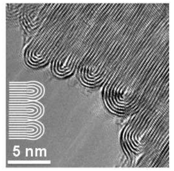

PCNF-B-G-NA : Edge

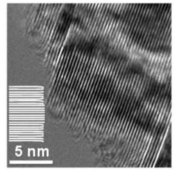

Effect of edge and basal surfaces on the SEI formation

< First cycle >

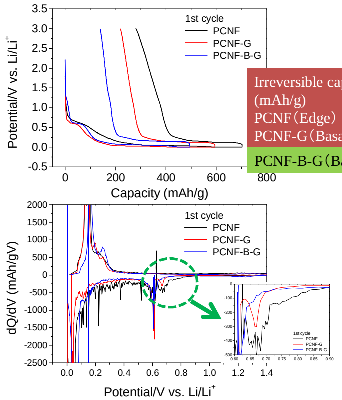

Irreversible capacity (mAh/g)
PCNF(Edge) : 281
PCNF-G(Basal) : 219
PCNF-B-G(Basal) : 139

< Second cycle >

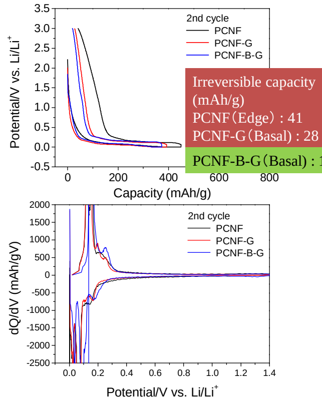

Irreversible capacity (mAh/g)
PCNF(Edge) : 41
PCNF-G(Basal) : 28
PCNF-B-G(Basal) : 19

Electrolyte : 1 M $LiClO_4$ in EC/DEC (1:1 vol%), Binder : PVDF 61

Effect of edge and basal surfaces on the SEI formation

PCNF : Edge

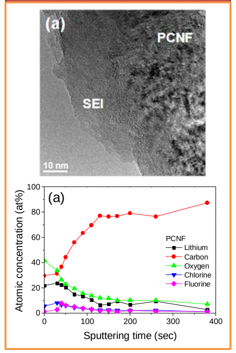

PCNF-G : Basal

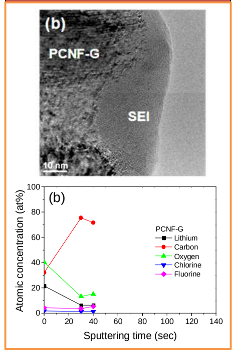

PCNF-B-G : Basal

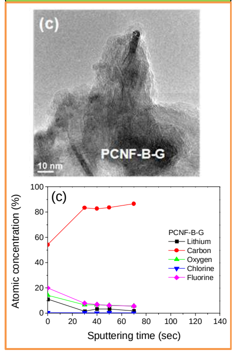

The XPS depth profiles indicated that the SEI of PCNF with edge surfaces was four times thicker than those of PCNF-G and PCNF-B-G with basal surfaces.

62

Effect of boron doping on the SEI formation

< First cycle >

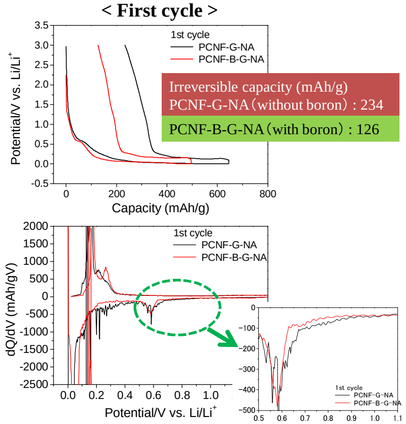

Irreversible capacity (mAh/g)
PCNF-G-NA(without boron) : 234
PCNF-B-G-NA(with boron) : 126

< Second cycle >

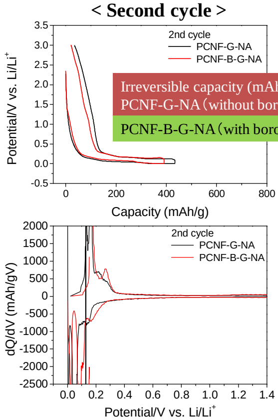

Irreversible capacity (mAh/g)
PCNF-G-NA(without boron) : 34
PCNF-B-G-NA(with boron) : 21

63

Effect of boron doping on the SEI formation

PCNF-G-NA : Edge

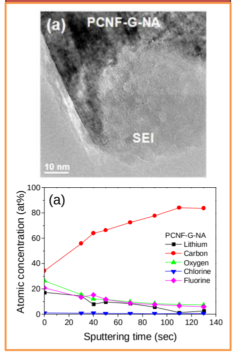

PCNF-B-G-NA : Edge

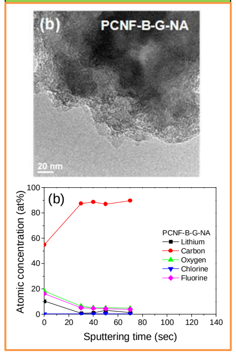

The SEI of PCNF-G-NA without boron doping was three times thicker than that of PCNF-B-G-NA with boron doping.

64

Explosion accident of Li-ion battery for EV (GM) 2012,04,12

GM Worker Injured After Lithium-Ion Battery Explodes